25th ABCM International Congress of Mechanical Engineering
October 20-25, 2019, Uberlândia, MG, Brazil

COB-2019-0413
EFFECTS OF SUPERFICIAL SHEAR STRESS ON STRATIFIED FLOW DYNAMICS IN A NARROW RECTANGULAR CHANNEL

Luciano Azeredo Merlo
Renato do Nascimento Siqueira
Michel de Oliveira dos Santos
Instituto Federal do Espírito Santo, Department of Mechanical Engineering,
Rod. BR 101 Norte, km 58, Litorâneo, São Mateus, Espírito Santo, Brazil.
lucianomerlo41@gmail.com
renatons@ifes.edu.br
michel.santos@ifes.edu.br

Abstract. *There is a growing need for good management of water resources and alternatives for effluents treatment. Given the fact, to improve the management of water bodies such as rivers, estuaries and coastal waters, it is necessary to understand the mixing mechanisms present in such environments. Numerical simulations were conducted with different levels of stratification to evaluate their effect on mixing and transport processes in a narrow rectangular channel. The main flow characteristics, such as corner flow and the decrease of the maximum velocity level, were affected by stratification. The same conditions and geometry were applied, also using Computational Fluid Dynamics (CFD), assuming a shear stress distribution on the surface as boundary condition. It was verified the necessity to define the stresses that act on the water surface, since they change the flow dynamics in the open channel. The main phenomena inherent to the analyzed flow were well reproduced when compared to experimental data, showing the potential of this tool to evaluate the conditions under different levels of stratification. Once calibrated, a CFD model is useful to understand the effects of stratification on turbulent flow behaviour and it can contribute to study environmental pollution in water bodies as well as to improve the performance of industrial processes in which stratification is present.*

Keywords: *Stratified flow, Free surface, Computational Fluid Dynamics (CFD).*

1. INTRODUCTION

The increasing urbanization of the cities, followed by the consequent increase in number of industries and the population, are some factors that highlight the concern about the use of water, as well as the final destination of the produced effluents. Therefore, new management policies for water bodies, such as rivers, estuaries and coastal waters, have been implemented aiming a better use of these resources. In order to improve such management, scientists and engineers have focused on understanding the mixing mechanisms present in these environments.

The transport and mixing mechanisms in turbulent flows are very complex. In many cases of practical importance, such as estuarine flows (which can be considered narrow channels when subjected to aspect ratio (width to depth ratio) smaller than 3), the situation can become even more complex due to stratification, which reduces the vertical mixing of solutes. Some other phenomena can also affect directly the flow dynamics, like the corner flow (Siqueira, 2002).

In many situations where the channel flow is found, in nature or artificial project, the surface is free to the atmosphere. Nezu and Rodi (1985) were one of the pioneers to measure secondary flows in open channels. They verified that the secondary flows, induced by turbulence anisotropy due the wall effects, transfer momentum from the surface to the bottom of the channel following the symmetry line, making the maximum velocity not located on the surface but below it, featuring a phenomenon called the velocity-dip which is peculiar to narrow channels.

Speziale (1987) describes the corner flow like a phenomenon that occurs due to secondary flows with high momentum that transports the fluid from the central region to the corners of the channel, causing distortion of the longitudinal velocity contour.

The modeling of the surface have been a challenge to many researchers due to de presence of shear stress at this region that affect directly the development of the velocity profile. The simplest approach to implement in a CFD model is a symmetry plane condition that implies in a null stress in this region (Tang and Crossley, 2005). However, typically in narrow channels, velocity gradients cannot be negligible due to the velocity dip presence. Thus, this work evaluate the influence of the superficial stress on the flow dynamic, in order to ascertain the importance of a better definition of the surface condition in open channels.

Although there are many significant results about the effects of stratification on mixing and transport processes, the topic is still not conclusive and new researches must be done. This work also investigates, using a Computational Fluid Dynamic approach, the mixing and transport effects due to the increasing of stratification level in a narrow rectangular channel flow with free surface.

1.1 Governing equations

Using the Reynolds decomposition over the instantaneous values from the governing flow equations, the following continuity, momentum and solute transport equations written, respectively, in indicial notation are obtained in function of averaged quantities:

Continuity equation:

$$\frac{\partial U_i}{\partial x_i} = 0 \tag{1}$$

Where U_i is the time averaged velocity in the x_i direction, considering a incompressible and steady state flow.

Momentum equation:

$$\frac{\partial U_i}{\partial t} + U_j \frac{\partial U_i}{\partial x_j} = -\frac{1}{\rho_r}\frac{\partial P}{\partial x_i} + \frac{\partial}{\partial x_j}\left(\nu \frac{\partial U_i}{\partial x_j} - \overline{u_i u_j}\right) + g_i \frac{\rho - \rho_r}{\rho_r} \tag{2}$$

U_j is the time-averaged velocity in the x_j direction, ρ is the time-averaged density, P is the static pressure and ν is the molecular viscosity. The buoyancy effects are only taken into account by the last term in the right hand side of momentum equation, which involves the reference density (ρ_r) and the gravitational acceleration (g_i) in the (x_i) direction. *U* is the time-averaged velocity, *i* and *j* are the dummy index for indicial notation, representing the rectangular directions (axial when index equals 1, transverse when equals 2, vertical when equals 3), where *i* is different than *j*.

Solute transport equation:

$$\frac{\partial C}{\partial t} + U_i \frac{\partial C}{\partial x_i} = \frac{\partial}{\partial x_i}\left(\Gamma \frac{\partial C}{\partial x_i} - \overline{u_i c}\right) + S_C \tag{3}$$

Where Γ is the molecular diffusivity, *C* is the mean solute concentration, u_i and *c* are the fluctuating velocity and solute concentration, respectively. S_C is a source term, which can represent, for instance, a release of solute into the system or its decay due to a chemical reaction. Due to the decomposition process, unknown correlations between the fluctuating velocities ($\overline{u_i u_j}$) and between velocity and concentration fluctuations ($\overline{u_i c}$) appear in the momentum and solute transport equations, respectively. Therefore, a turbulence model was necessary to be introduced.

The Baseline Reynolds Stress (BSL) was used to represent the closure problem of the governing flow equations because, since the dynamics of the flow in a narrow channel suffers strong influence of the wall (Chaudhuri and Sahoo, 2018; Flores and Jimenez, 2006), a good definition of the outflow phenomena close to this region is required. The application of such a model allows a flexible grid resolution near the wall. The main equations that represent the applied turbulence model are described by Eq. (4) and Eq. (5).

$$\frac{\partial(\rho k)}{\partial t} + \frac{\partial(\rho k u_i)}{\partial x_i} = \frac{\partial}{\partial x_j}\left(\Gamma_k \frac{\partial k}{\partial x_j}\right) + G_k - Y_k + S_k \tag{4}$$

$$\frac{\partial(\rho \omega)}{\partial t} + \frac{\partial(\rho \omega u_j)}{\partial x_j} = \frac{\partial}{\partial x_j}\left(\Gamma_\omega \frac{\partial \omega}{\partial x_j}\right) + G_\omega - Y_\omega + D_\omega + S_\omega \tag{5}$$

In these equations, the term G_k represents the production of turbulence kinetic energy and G_k represents the generation of ω. Γ_k and Γ_ω represent the effective diffusivity of *k* and ω, respectively. Y_k and Y_ω represent the dissipation of *k* and ω due to the turbulence. D_ω represents the cross-diffusion term and, finally, S_k and S_ω are user-defined source terms.

The expression that describe the shear stresses are represented respectively by Eq. (6), where the first and second indexes indicates the plan and the direction, respectively.

$$\tau_{ij} = \rho \overline{u_i u_j} \tag{6}$$

2. METHODOLOGY

2.1 Solution parameters

The software used was the CFX® version 16.0, a commercial software commonly used for fluid dynamics simulation. The geometry and the inlet conditions used in the simulation were based on Siqueira (2002) experimental studies, who evaluates the effects of stratification on the transport and mixing processes in narrow rectangular channels. The experimentally evaluated channel consists of two rectangular ducts that, when developing the flow profile, enter the main channel, where the transport and distribution processes will occur. The stratification levels were varied as the concentration of the aqueous salt solution of the lower inlet duct.

At first, the channel inlet was numerically modeled in order to develop a velocity profile to be inserted as inlet condition in the main channel. The same velocity profile was applied to the two main channel inlets. It consists in a rectangular duct and its dimension of length, width and height are 2.5 m, 0.05 m and 0.1 m, respectively. Tab. 1 presents the conditions applied to this simulation.

Table 1. Conditions applied to the inlet rectangular duct simulation.

Default Domain	Turbulence model	BSL Reynolds Stress
Boundary conditions	Inlet	Velocity = 0.25 m/s
	Outlet	Null relative pressure
	Wall	No slip condition
	Symmetry	Null velocity gradient
Solver control	Timescale factor	0.1
	Residual target	1e-5

Nezu and Nakagawa (1993) and Cruz et al. (2019) presented the main phenomena inherent to the flow dynamics in a narrow rectangular duct. Satisfactory results in the outlet section were obtained with respect to the distorted longitudinal contours due to the presence of the secondary currents coming from the turbulence anisotropy, allowing its use as contour condition at the entrance of the main channel, where the transport processes and mixing of solutes.

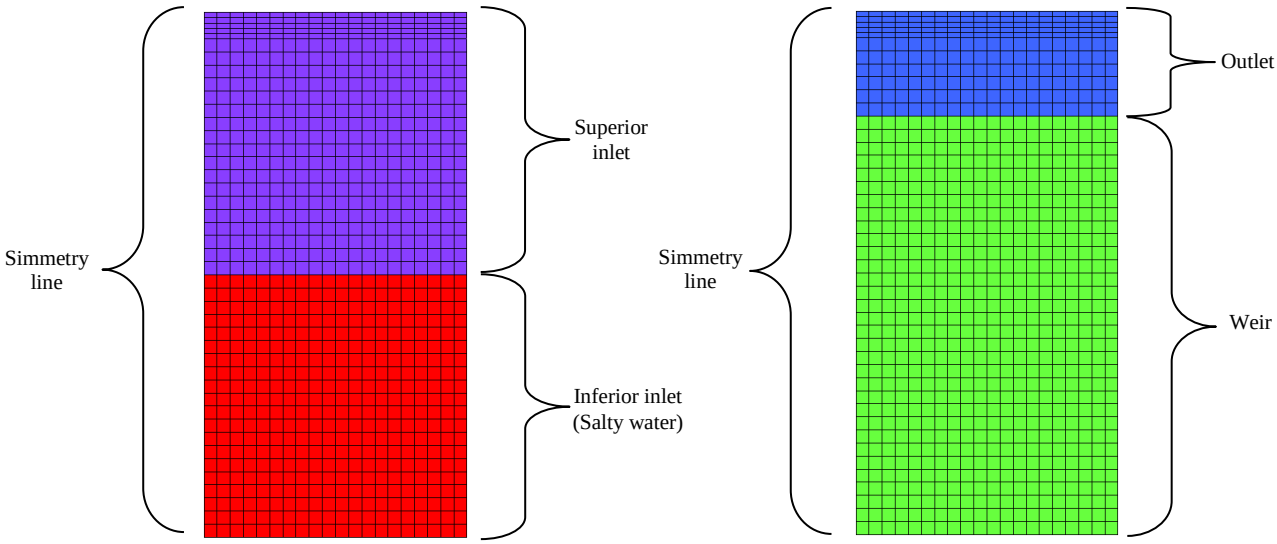

a) Inlet section of the main channel. b) Outlet section of the main channel.

Figure 1. Inlet and outlet sections of the main channel presenting the layout of the mesh used in the main channel simulations.

The modeling of the main channel was done making the geometry with the same dimensions used in the experimental bench. The values attributed to the length, width and height of the water volume are 9.5m, 0.05m and 0.1m, respectively. A 0.08m high weir, calculated based on Delmee (2003), was used to the channel outlet to keep the fluid level constant throughout the entire channel. A computational mesh with 3.8e+6 elements was generated based on the more refined grid close to the surface. Fig. 1 illustrates the mesh applied to the present study.

At the domain setup, the baseline turbulence model (BSL) was used because it was observed a better behaviour of the flow next to the wall and most accurate corner flow effects generated by the secondary currents. The production and dissipation of turbulence kinetic energy were assumed based in the average of the data presented by Siqueira (2002) and the CFX default (because it takes into account the gradient of solute concentration), respectively. The stratification level (*DDi*) was represented by the specific mass difference between the water with solute and the pure water. The surface was considered, at first, like a wall with free slip condition, according to many researchers. After, the shear stress expressions was applied to this region to verify their influence on the flow dynamics.

By means of the experimental data available by Siqueira (2002) of the tensions located near the surface region in the dimensionless longitudinal position x_1/Dh=48, expressions were made to be used as boundary condition for this region. First, a regression was performed that best represented the values of the efforts in the transverse direction. Then, such a polynomial was assigned to a logarithmic longitudinal distribution, starting from the main channel inlet to the data acquisition section. Finally, assuming that, from this section, the flow would be fully developed, the transverse distribution was taken as constant until reaching the outlet.

Using the conditions cited, it was performed two main modeling: a non-stratified flow (*DDi* = 0 kg/m³) and a stratified case, with stratification level equal to 5 kg/m^3, keeping others boundaries conditions constant. All the sections analyzed were localized at 6.4 m from the inlet and the variables of position (transverse and vertical) and velocity (in longitudinal direction) was dimensionless based on the total height (*H*), total width (*B*) and average velocity (*U*), respectively. For each case, it was simulated with free slip condition at the surface and, after, with de shear stress expressions obtained for comparison purpose. The Tab. 2 presents the conditions applied to the main channel simulation.

Table 2. Conditions applied to the main channel simulation.

Default Domain	Turbulence model	BSL Reynolds Stress
	Turbulent Schmidt Number	0.9
	Kinematic Diffusivity	1.35e-5 cm²/s
Boundary conditions	Superior inlet	Developed velocity profile Salty water mass fraction = 0
	Inferior inlet	Developed velocity profile Salty water mass fraction = 1
	Outlet	Null relative pressure
	Surface	Free slip condition or Shear Stress expressions
	Wall	No slip condition
	Symmetry	Null velocity gradient
Solver control	Timescale factor	0.1
	Residual target	1e-5

3. RESULTS

3.1 Shear stress expressions

The superficial shear stress expressions applied in the top boundary condition to the non-stratified case (DDi=0kg/m³) are presented on Eq. (7) and Eq. (8) in function of transverse (x_2) and longitudinal (x_1) positions. *Dh* represents the hydraulic diameter and it is calculated by the ratio between four times the transversal section area and the wet perimeter.

$$\tau_{32} = \begin{cases} -0.1635\cdot(168.718{x_2}^2 + 8.1906x_2 - 0.0244) & \text{if } x_1 > 6.4\text{m} \\ -0.1635\cdot(168.718{x_2}^2 + 8.1906x_2 - 0.0244)\cdot\left(\dfrac{x_1}{48\cdot Dh}\right)^{\frac{\ln(0.50)}{\ln(0.90)}} & \text{if } 0 \le x_1 \le 6.4 \end{cases} \quad (7)$$

$$\tau_{31} = \begin{cases} 0.1635 \cdot (227.37 x_2{}^2 + 23.026 x_2 - 0.3323) & \text{if } x_1 > 6.4\text{m} \\ 0.1635 \cdot (227.37 x_2{}^2 + 23.026 x_2 - 0.3323) \cdot \left(\dfrac{x_1}{48 \cdot Dh} \right)^{\frac{\ln(0.50)}{\ln(0.90)}} & \text{if } 0 \le x_1 \le 6.4 \end{cases} \quad (8)$$

Similarly, the superficial shear stress expressions used in the top boundary condition to the stratified case (for *DDi*=5kg/m³) are represented by the Eq. (9) and Eq. (10).

$$\tau_{32s} = \begin{cases} 0.1635 \cdot (-4209.9 x_2{}^3 + 511.03 x_2{}^2 - 16.666 x_2 + 0.1009) & \text{if } x_1 > 6.4\text{m} \\ 0.1635 \cdot (-4209.9 x_2{}^3 + 511.03 x_2{}^2 - 16.666 x_2 + 0.1009) \cdot \left(\dfrac{x_1}{48 \cdot Dh} \right)^{\frac{\ln(0.50)}{\ln(0.90)}} & \text{if } 0 \le x_1 \le 6.4 \end{cases} \quad (9)$$

$$\tau_{31s} = \begin{cases} 0.1635 \cdot (9418.6 x_2{}^3 + 778.46 x_2{}^2 - 13.438 x_2 + 0.0474) & \text{if } x_1 > 6.4\text{m} \\ 0.1635 \cdot (9418.6 x_2{}^3 + 778.46 x_2{}^2 - 13.438 x_2 + 0.0474) \cdot \left(\dfrac{x_1}{48 \cdot Dh} \right)^{\frac{\ln(0.50)}{\ln(0.90)}} & \text{if } 0 \le x_1 \le 6.4 \end{cases} \quad (10)$$

3.2 Shear stress effects on flow dynamics

Fig. 2 shows the velocity profile for the non-stratified case. In Fig. 2b, it can be observed that the free slip condition applied to the surface changed the velocity contours when compared to the experimental data of Siqueira (2002) represented in Fig. 2a. In the absence of stresses in this region, there is a smaller distortion effect in the contours governed by the secondary currents, carrying lower momentum to the central region of the channel. On the other hand, Fig. 2c shows that the longitudinal velocity profile is best represented, since the shear stresses on the surface are defined. It can also be observed the better accuracy of the occurrence of velocity dip, where the maximum velocity level in the flow is below the surface level, in z/H = 0.6, or 60% of the height of the water slide. There is little influence of surface tensions in the lower channel region, remaining typical distortions from the corner flow.

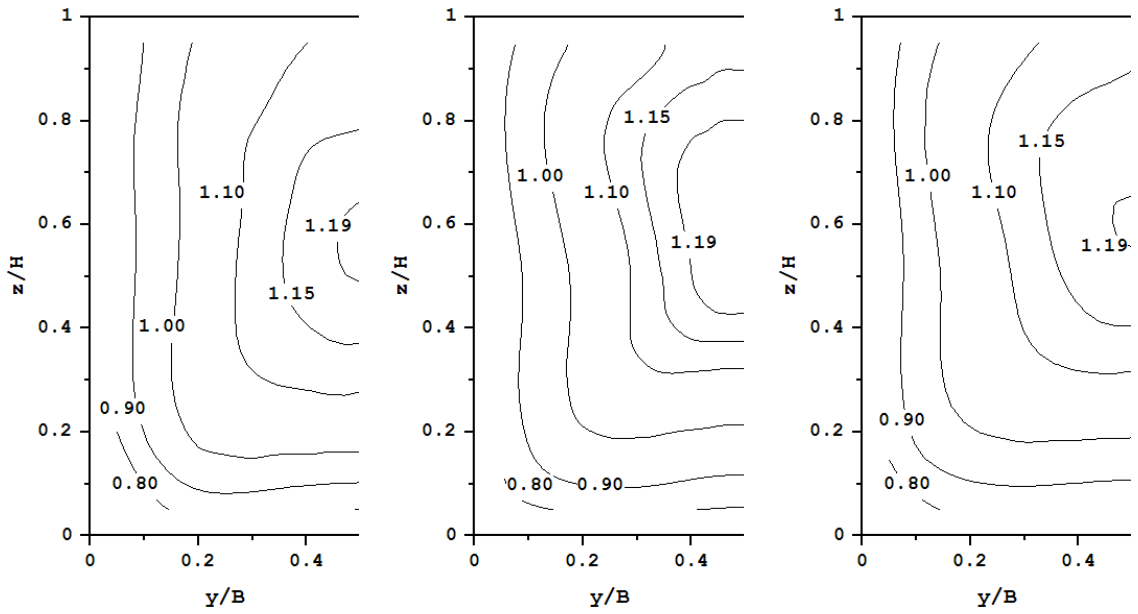

a) Experimental result (Siqueira, 2002). b) Free-slip condition. c) Shear stress condition.

Figure 2. Main velocity in the longitudinal direction for the non-stratified flow case at the section x/Dh=48 and density difference DDi=0kg/m³.

As seen in Fig. 3, the lower vortices are bounded by the bottom of the channel, while the upper vortices are much more intense and extend to the surface. When approaching the water surface, the secondary currents transfer momentum from the region near the wall to the center of the channel. Then, when reaching the central limit, they are redirected

towards the symmetry line, maintaining the recirculation, which is the main factor causing the velocity dip phenomenon. One can also verify the strong influence of the secondary currents on the main velocity contours, where there is a more intense distortion of the contours in the region where the corner flow occurs.

The secondary flow were better represented when the shear stress expressions were applied. As illustrated in the Fig. 3c, the corner flow intensity had more accuracy when compared to experimental (Fig. 3a), while the simulation with free slip condition (Fig. 3b) overestimated the intensity of the occurrence of the phenomenon, culminating in a greater distortion of the velocity contours.

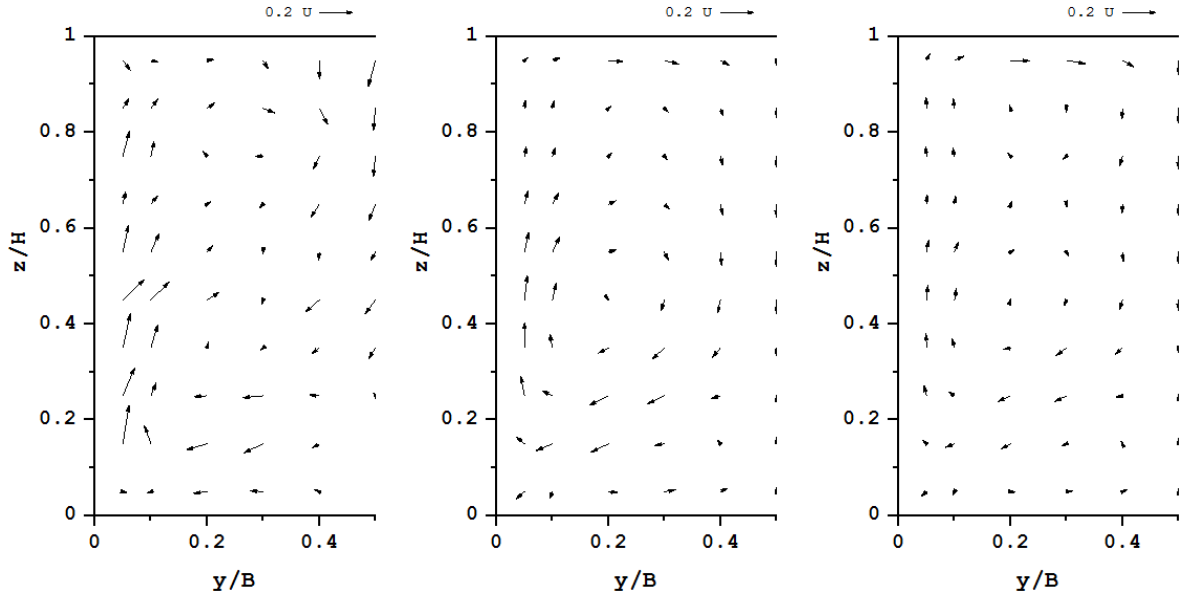

a) Experimental result (Siqueira, 2002) b) Free slip condition c) Shear stress condition

Figure 3. Secondary flow in the longitudinal direction for the stratified flow case at the section x/Dh = 48 and density difference DDi = 0kg/m³.

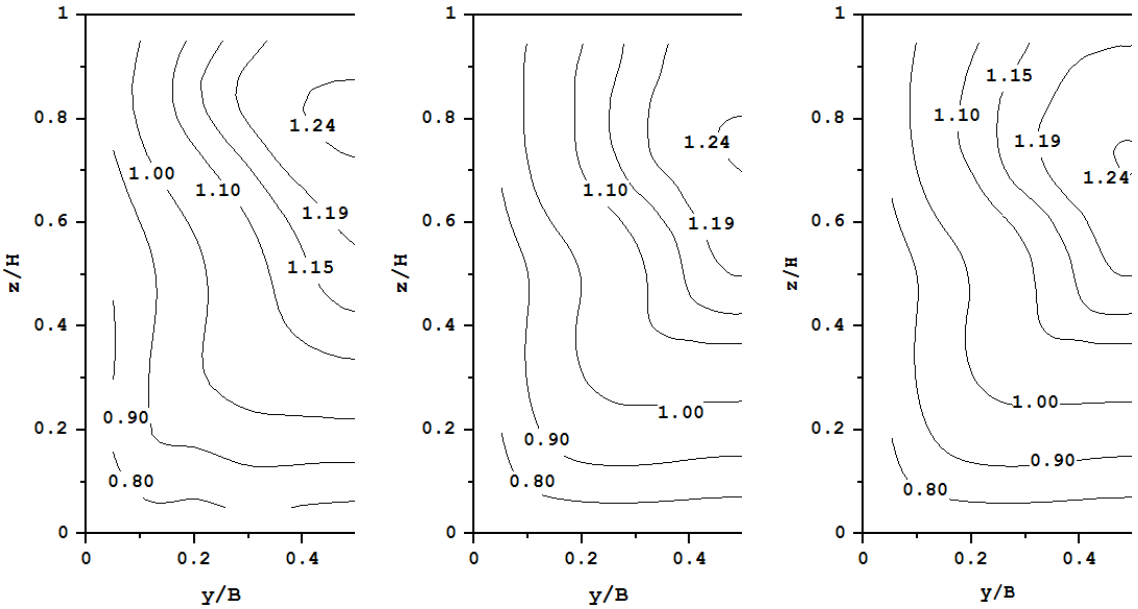

a) Experimental result (Siqueira, 2002) b) Free-slip condition c) Shear stress condition

Figure 4. Main velocity in the longitudinal direction for the stratified flow case at the section x/Dh=48 and density difference DDi=5kg/m³.

For the stratified case (Fig. 4), typical characteristics of this kind of flow can be seen, such as the decrease in velocity dip intensity, which happened in about 80% of the total height. The event occurs because in this channel

section, the secondary downward movement in the central position (which is responsible for the formation of velocity dip) is still in development. This means that the stratification delays the development of the profiles due to reduction of vertical mixing, by the action of the buoyancy forces originated by the concentration gradients. It is possible to reaffirm a better definition of flow patterns when modeling is performed with definition of shear stress profile in the surface, as illustrated in the Fig. 4c. In the absence of this effort (Fig. 4b), near surface, low momentum is carried to the central region of the section. Consequently, the desired deformation of the velocity contour was not obtained.

Fig. 5 illustrates secondary flow, given the increase in stratification level. It is possible to notice a greater intensity of the transfer of momentum in the inferior region of the channel, when compared to the flow in the absence of a density difference (Fig. 3). Such phenomenon is mainly responsible for the decrease in the velocity dip effect. A greater secondary flow accuracy is also verified in the simulation with shear stress condition, as presented in the Fig. 5c, when compared to the experimental results (Fig. 5a).

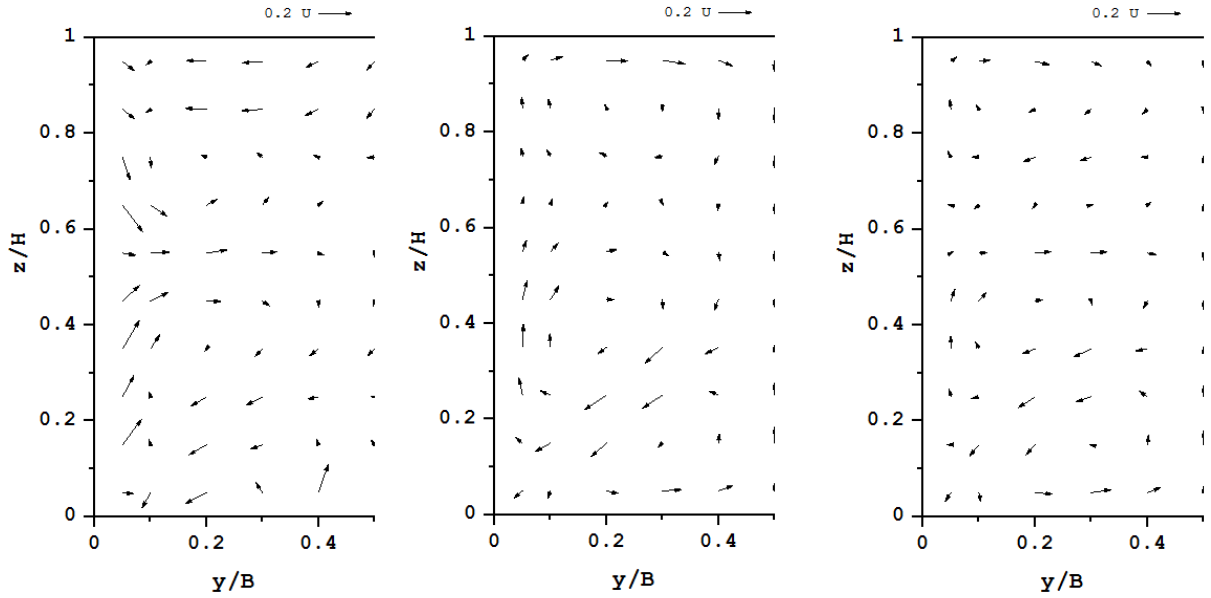

a) Experimental result (Siqueira, 2002) b) Free-slip condition c) Shear stress condition

Figure 5. Secondary flow in the longitudinal direction for the stratified flow case at the section x/Dh=48 and density difference DDi=5kg/m³.

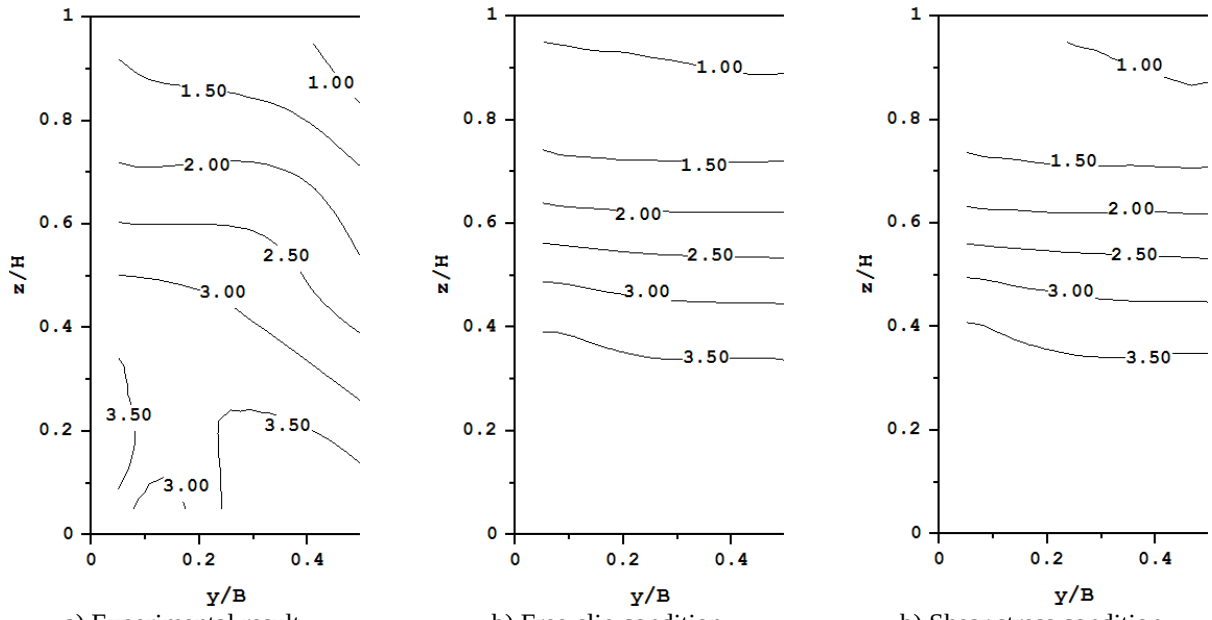

a) Experimental result b) Free-slip condition b) Shear stress condition

Figure 6. Density distribution at the section x/Dh = 48 and density difference DDi = 5kg/m³.

Fig. 6 presents a strong influence of the secondary flow on the density gradient distribution. It can be observed that, where the secondary flow has greater magnitude, due to the presence of the corner flow (mainly next to the wall), the mixing processes are more intense. It can also be observed that when shear stresses are inserted in the surface (Fig. 6c), the density distribution contours are better defined in the superior region of the channel when compared to the experimental one (Fig. 6b), since there is a greater momentum transfer directed from surface to simmetry line. Consequently, a higher mixing gradient occurs when compared to the case where surface effects are neglected (Fig. 6c).

4. CONCLUSIONS

The main flow characteristics for the non-stratified flow simulation such as corner flow and velocity dip, was well represented and permit to comprehend the phenomena which directly affect the dynamic of the transport and mixing processes in rectangular channels. It was observed that the addition of stratification level is straightly related to the decrease of velocity dip. Besides, it is relevant to note the importance to consider the shear stress on free surface, since in this region the velocity gradients cannot be considered null. The insertion of the expressions representing the shear stresses on the surface provided a better accuracy with respect to the main phenomena present in open channel rectangular channels. The comprehension of the studied mechanisms is a step for the development of better management tools of hydric resources, reducing the impact of effluent release in water bodies such as estuaries and increasing the industrial processes efficiency.

5. ACKNOWLEDGEMENTS

The authors thank the Instituto Federal do Espírito Santo *Campus* São Mateus for the structure and support during the development of this work.

6. REFERENCES

Chaudhuri, S., Sahoo, S., 2018. “Effect of the aspect ratio on the flow characteristics of magnetohydrodynamic (MHD) third grade fluid flow through a rectangular channel”. *Indian Academy of Sciences*, pp 1-10.

Cruz, M.A., Thompson, R.L., Bacchi, R.D., Sampaio, L.E.B., 2019. “The use of the Reynolds force vector in a physics informed machine learning approach for predictive turbulence modeling”. pp 1-25.

Delmée, G. J., 2003. *Manual de medição de vazão*. Edgard Blucher Ltda, São Paulo, 3rd edition.

Flores, O., Jimenez, J., 2006. “Effect of wall-boundary disturbances on turbulent channel flows”. *Journal of Fluid Mechanics*, Vol. 566, pp. 357-376.

Nezu, I., Nakagawa, H., 1993. *Turbulence in open-channel flows*. IAHR Monograph, A. A. Balkema, Rotterdam, Brookfield.

Nezu, I., Rodi, W., 1985. “Experimental study on secondary currents in open channel flow”. In *Proceedings of the 21st IAHR Congress*. Melbourne, Australia.

Siqueira, R.N., 2002. *Transport and mixing processes in stratified flow*. Ph.D. thesis, Loughborough University, Loughborough, England. 2002.

Speziale, C.G., 1987. “On nonlinear K-l and K-ε models of turbulence”. *Journal of Fluid Mechanics*, Vol. 178, pp. 459-475.

Tang, X., Croslley, A.J., 2005. “Guidelines for applying commercial CFD software to open channel flow”. 15th Jul. 2019. < https://www.nottingham.ac.uk/cfd/ocf/Methodology.pdf>.

7. RESPONSIBILITY NOTICE

The authors are the only responsible for the printed material included in this paper.